SAND2016-2515C

Temperature and oxygen measurements in a metallized propellant flame by hybrid fs/ps rotational coherent anti-Stokes Raman scattering

Sean P. Kearney and Daniel R. Guildenbecher
Engineering Sciences Center, Sandia National Laboratories, PO Box 5800, Mail Stop 0824, Albuquerque, NM 87185 USA
Author e-mail address: spkearn@sandia.gov

Abstract: Ultrafast pure-rotational CARS is applied to an aluminized ammonium-perchlorate propellant flame. Background-free spectra were acquired in this challenging high-temperature, particle-laden environment and successfully fit for temperature and oxygen/nitrogen ratio using a simple theoretical model.
OCIS codes: (120.1740) Combustion diagnostics; (120.6780) Temperature; (300.6230) Spectroscopy, coherent anti-Stokes Raman scattering

1. Introduction

Metals, such as aluminum, are frequently added to solid propellants to enhance specific impulse and improve combustion stability. When a metalized propellant burns, surface flame temperatures are often sufficient to melt the micron-sized metal particles and loft them into the flame, where they can form large-scale agglomerates that reach hundreds of microns in diameter. Laser-based diagnostics [1] represent some of the most promising methods for spatially and temporally resolved thermochemical data in combustion, but optical probing of metal-particle-laden flames for temperature and species is particularly complicated by scattering and radiative emission by the hot metal particles. For example, the 6-mm diameter ammonium perchlorate (AP) propellant strand investigated here is shown in Figure 1. White-hot emission from aluminum particulate and the associated smoke are readily seen and represent a significant challenge for optical diagnostics.

2. Experiment

CARS spectra were acquired using the rotational fs/ps CARS facility described in detail in [2] and briefly summarized here. A single-box Ti:sapphire chirped-pulse amplifier (Spectra Physics "Solstice") delivered a 1-kHz train of 800 nm, 90-100 fs pulses with a nominal bandwidth of 190 cm^{-1} (FWHM). Eighty percent of the 3.1-mJ pulse energy was used to generate a 1−1.4 mJ, 5-ps-duration probe pulse at 400 nm, using the Second-Harmonic-Bandwidth-Compression (SHBC Light Conversion) approach described in [2]. The spectral width of the probe laser beam was 3.5 cm^{-1} (FWHM). The remaining 20% of the compressed 800-nm femtosecond pulse was sent through a time of flight delay and split 50/50 to form separate pump and Stokes pulses, whose energies were regulated to ~100 μJ/pulse by a variable attenuator. Computer-controlled delay lines adjusted the relative path lengths of all three laser pulses to ensure proper sequencing in time. A 50-60 fs delay between the pump and Stokes pulses was introduced to optimize the performance of the CARS system at high temperatures, using the spectral focusing approach described in [3]. The 5-ps probe pulse was delayed by τ = 16 ps with respect to the pump/Stokes preparation pulses to provide time-gated elimination of any nonresonant CARS response [4]. The three laser beams were arranged in a planar crossed-beam phase-matching scheme, and a f = 500-mm beam-crossing lens was employed to generate the CARS signal beam in a nominally ellipsoidal measurement volume, with ~100-μm minor axis, and a major axis in which

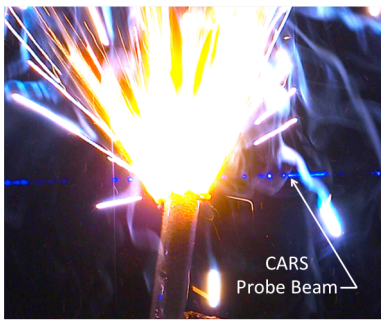

Fig. 1. Aluminized AP propellant flame with 400-nm CARS probe beam.

90% of the CARS signal was generated in a 1.8-mm axial beam overlap region. The CARS signal was dispersed at ~0.5 cm^{-1}/pixel onto a back-illuminated, electron-multiplying CCD camera by a 1-m grating spectrograph with a grating groove density of 1800 mm^{-1}. Mie scattering of the probe laser line by large aluminum particles was particularly intense and was minimized, although not eliminated, using apertures and a dielectric edge filter (Semrock "Razor Edge") [5] with a fast rise from the cutoff to the pass band in < 20 cm^{-1}.

An aluminized propellant, nominally 70% ammonium perchlorate (AP), 20% aluminum particulate, and 10% hydroxyl terminated polybutadiene binder, was formed into a pencil-like strand that was roughly 6-mm in diameter and 100-mm in length. Detailed characterization of the aluminum particulate in these burning propellant samples has been provided via digital in-line holography (DIH) using the methods discussed by Guildenbecher *et al.* [6]. The DIH data revealed aluminum agglomerates that ranged from ten to several hundreds of microns.

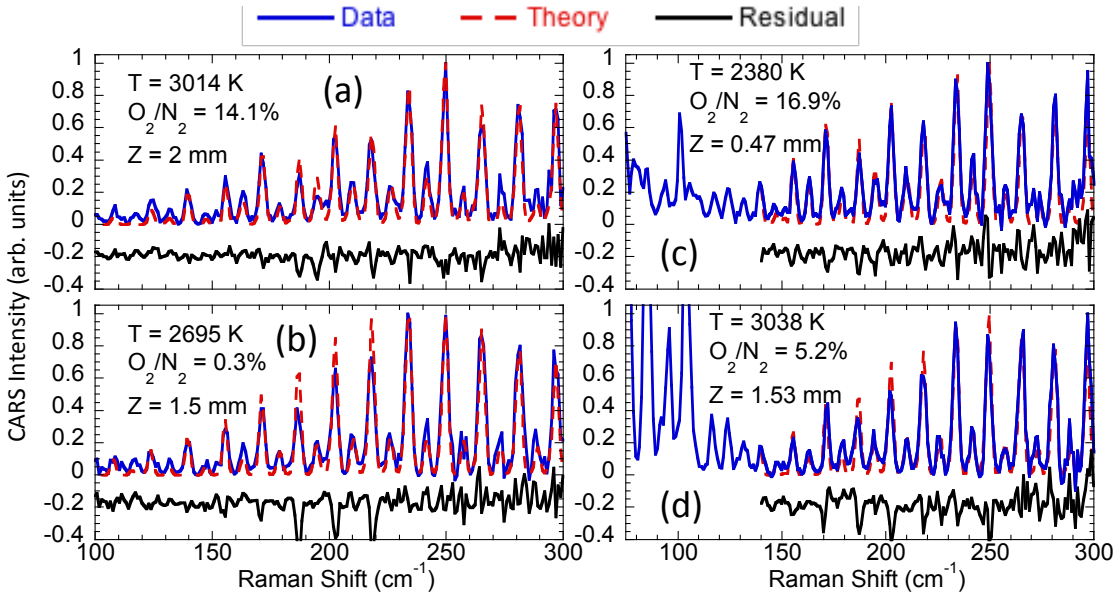

Fig. 2. Single-laser-shot rotational CARS spectra from the aluminized ammonium perchlorate flame.

3. Results and Discussion

Single-laser-shot rotational fs/ps CARS spectra were acquired with a probe-pulse delay of τ = 16 ps for approximately 60 seconds following ignition for two different propellant strand burns. During the first 10 seconds (8 mm of surface regression) approximately 80% of the spectra displayed detectable signal-to-noise, defined here as peak detector counts of 500 or more above background. Signal dropout during the remaining 20% of the laser shots presumably arose as a result of beam-steering effects and/or low signal levels resulting from the extremely high temperatures encountered near the burning propellant surface.

Representative single-laser-shot CARS spectra are shown along with the best-fit theoretical prediction and associated temperature and O_2/N_2 ratio in Figure 2. The spectra are free of nonresonant background, which has been observed to overwhelm the Raman-resonant signal in CARS spectra obtained from aluminum-particle-seeded flames, and to similarly dominate spectra obtained with the present setup at zero probe delay [7]. This time-gated elimination of the nonresonant contribution is a key feature of the ultrafast fs/ps technique and enables CARS probing of metal-particle-laden flames, which has not previously been possible. CARS intensities at Raman shifts below ω = 100 cm^{-1} were frequently impacted by intense scattering of the probe laser line by particulate, which was sufficiently strong to compete with the low-frequency portion of the CARS spectrum in-spite of the dielectric edge filter employed. The measured spectra could generally be classified as resulting from high-temperature gas only, as shown in Figure 2a and b, or from both hot and cold gases simultaneously as a result of high thermal gradients along the 1.8-mm axis of the measurement volume, as in Figure 2c and d. The effect of thermal gradients within the CARS measurement volume has been reported for nanosecond CARS spectra [8], where the cold-gas signal at low Raman shifts dominates the spectrum, with weaker intensity contributions from hot gases present at higher frequency. Spectra that were determined to be impacted by gradients were fit using the hot-gas-dominated, high-frequency portion of the spectrum, with Raman shifts ω = 140 − 300 cm^{-1}, in order to achieve a result that was indicative of

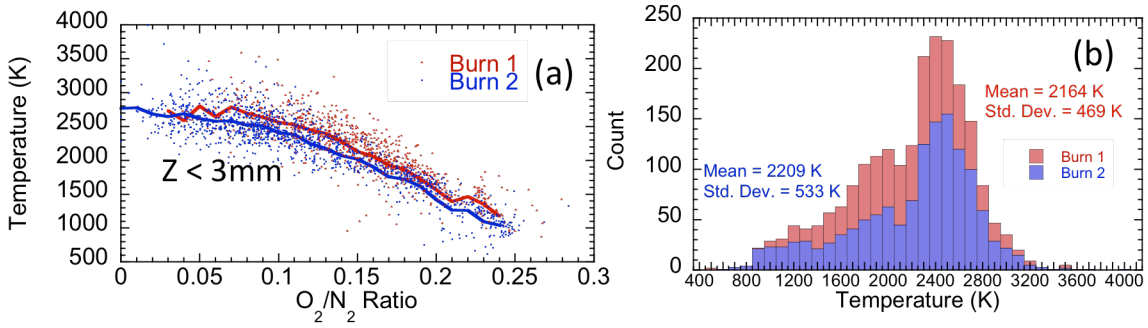

Fig. 3. Temperature/oxygen scatter plot (a); histogram of temperature fluctuations (b). Data have been compiled from two different aluminized ammonium perchlorate burns.

the highest temperatures in the measurement volume. Spectra determined to be largely unimpacted by thermal gradients were fit using a wider spectral region of $\omega = 100 - 300$ cm^{-1}.

Significant O_2 content could be observed at times throughout the duration of the propellant burns. This was true even early in the experiments, when the CARS measurement volume was positioned close to the surface, so that mixing with room air was likely minimized, and the temperatures were very high, in excess of 2500 K. Indeed, the spectrum shown in Figure 2a reveals a fit temperature of $T = 3014$ K with a significant O_2/N_2 mole-fraction ratio of 14.1%. This contrasts what is observed in more common hydrocarbon/air combustion, where O_2 is rapidly consumed as temperature increases. In the case of AP combustion, O_2 can be a significant product species [9] and may possibly be present even at temperatures in excess of 3000 K. The spectra shown in Figures 2b and c are indicative of two different scenarios at temperatures in the range $T \sim 2400-2700$ K. In Figure 2b, at $T = 2695$ K, very little O_2 is present, as indicated by the smoothly varying envelope formed by the peak intensities, perhaps indicating a scenario where O_2 has been consumed by products of AP or binder combustion. The spectrum in Figure 2c returns a similar fitted temperature to 5b (within 13%) but with a much higher O_2/N_2 ratio of 16.9%, as indicated by the significant variations in the spectral intensity envelope, and potentially indicative of O_2 product from the AP burn, or entrained oxygen, mixing with high-temperature AP products that do not consume oxygen.

Scatter plots of temperature vs. O_2/N_2 ratio were constructed from single-laser-shot measurements where the probe volume was within 3 mm (1/2 strand diameter) of the burning surface, with the results shown in Figure 3a. Data from two different burns are shown with conditionally averaged temperatures drawn as solid lines through the data scatter. The conditionally averaged temperatures for the two experiments agree to within 3−10% across the full range of O_2 content. These conditionally averaged temperatures trend toward zero O_2 content at high temperatures suggesting that oxygen is generally consumed in the atmospheric AP burn, but with significant scatter about the conditional mean as a result of the above-mentioned persistence of O_2 at elevated temperatures. Temperature probability densities for heights $z \leq 3$ mm from the burning surface were estimated based on histograms of the CARS-measured temperatures, with the results shown in Figure 3b. Mean temperatures for the two experiments are $T = 2164$ K and 2209 K, respectively, or within 2.1%. The shapes of the two temperature histograms are additionally quite similar, with the most probable temperature near $T = 2400 - 2450$ K.

References

1. A. C. Eckbreth, *Laser Diagnostics for Combustion Temperature and Species* (Gordon and Breach, 1996).
2. S. P. Kearney, "Hybrid fs/ps rotational CARS temperature and oxygen measurements in the product gases of canonical flat flames," Combustion and Flame **162**, 1748-1758 (2015).
3. S. P. Kearney, "Bandwidth optimization of femtosecond pure-rotational coherent anti-Stokes Raman scattering by pump/Stokes spectral focusing," Applied Optics **53**, 6579-6585 (2014).
4. T. R. Meyer, S. Roy, and J. R. Gord, "Improving signal-to-interference ratio in rich hydrocarbon–air Flames using picosecond coherent anti-Stokes Raman scattering," Applied Spectroscopy **61**, 1135-1140 (2007).
5. A. Bohlin, and P. E. Bengtsson, "Effective suppression of stray light in rotational coherent anti-Stokes Raman spectroscopy using an angle-tuned short-wave-pass filter," Applied Spectroscopy **64**, 964-966 (2010).
6. D. R. Guildenbecher, M. A. Cooper, W. Gill, H. L. Stauffacher, M. S. Oliver, and T. W. Grasser, "D. R. Guildenbecher, M. A. Cooper, and P. E. Sojka, "High speed (20 kHz) digital in-line holography (DIH) for transient particle tracking and sizing in multiphase flows," Applied Optics (in press) (2016)." Applied Optics (in press) (2016).
7. S. P. Kearney, and D. R. Guildenbecher, "Temperature measurements in metallized propellant combustion using hybrid fs/ps coherent anti-Stokes Raman scattering," submitted to Applied Optics (2016).
8. Y. Gao, T. Seeger, and A. Leipertz, "Development of temperature evaluation of pure Rotational Coherent Anti-Stokes Raman Scattering (RCARS) spectra influenced by spatial averaging effects," Proceedings of the Combustion Institute **35**, 3715-3722 (2015).
9. A. G. Keenan, and R. F. Siegmund, "Thermal Decomposition of Ammonium Perchlorate," Qaurterly Reviews - Chemical Society **23**, 430-452 (1969).